

Drill— Deep Reinforcement Learning for Refinement Operators in \mathcal{ALC}

Caglar Demir and Axel-Cyrille Ngonga Ngomo

Data Science Research Group, Paderborn University

Abstract. Approaches based on refinement operators have been successfully applied to class expression learning on RDF knowledge graphs. These approaches often need to explore a large number of concepts to find adequate hypotheses. This need arguably stems from current approaches relying on myopic heuristic functions to guide their search through an infinite concept space. In turn, deep reinforcement learning provides effective means to address myopia by estimating how much discounted cumulated future reward states promise. In this work, we leverage deep reinforcement learning to accelerate the learning of concepts in \mathcal{ALC} by proposing DRILL—a novel class expression learning approach that uses a convolutional deep Q-learning model to steer its search. By virtue of its architecture, DRILL is able to compute the expected discounted cumulated future reward of more than 10^3 class expressions in a second on standard hardware. We evaluate DRILL on four benchmark datasets against state-of-the-art approaches. Our results suggest that DRILL converges to goal states at least $2.7\times$ faster than state-of-the-art models on all benchmark datasets. We provide an open-source implementation of our approach, including training and evaluation scripts as well as pre-trained models.¹

Keywords: Deep Reinforcement Learning · Class Expression Learning

1 Introduction

Knowledge Graphs (KGs) represent structured collections of facts describing the world in the form of typed relationships between entities [16]. These collections of facts have been used in a wide range of applications including web search [12], question answering [3], recommender systems [37], cancer research [29], machine translation [27], and even entertainment [25].

In this work, we focus on the problem of Class Expression Learning (CEL) on RDF KGs as defined in [23]. CEL refers to the problem of learning Web Ontology Language (OWL) class expressions from a given background knowledge and examples [19]. Tackling CEL is particularly important as learned OWL class expressions can be transformed into natural language through verbalization [28] which makes predictions *ante-hoc explainable*. Ergo, optimizing CEL has the potential of easing the use of explainable AI in real-life applications along with the

¹ <https://github.com/dice-group/DRILL>

corresponding societal advantages tied to explainability [5,30]. The lack of transparency and explainability in AI systems reduces the trust and the verifiability of the decisions made [32,17,11,31].

The formal setting for CEL is as follows: Given background knowledge \mathcal{G} , a set of positive E^+ , and a set of negative examples E^- as well as a formal logic \mathcal{L} , the goal is to find a **class expression** H in \mathcal{L} such that $\mathcal{G} \models H(p) \wedge \mathcal{G} \models \neg H(n)$, where $p \in E^+$ and $n \in E^-$. This learning problem is often formulated as a search problem in a quasi-ordered state space (\mathcal{S}, \preceq) [4,20,14,15]. Within this setting, the CEL problem is tackled by learning a sequence of states that starts from an initial state (e.g., \top) and leads to a H , e.g., **Brother** \sqcup **Sister** in Example 1.

Example 1. Given a set of individuals who have siblings as E^+ and a set of only-children as E^- , a CEL approach could aim to learn **Brother** \sqcup **Sister**.

The search of H is steered by optimizing a heuristic function that aims to estimate how likely a state $s_i \in \mathcal{S}$ leading to H , ergo the heuristic value signals how well a class expression fits a learning problem and can be used to guide the search [19,20]. State-of-the-art approaches rely on heuristic functions that determine a heuristic value of s_i without any consideration for future states (see Section 3). This is akin to making decisions in a chess game solely based on the current board state and without any consideration for next possible board configurations. We argue that this is an important drawback of current CEL models, which leads to state-of-the-art models often needing to explore a large number of states to find satisfactory class expressions [2]. To remedy the problem of exploring a large number of states, a common practice is to apply (1) numerous handcrafted rules and/or (2) a reasoner to remove redundant states from the search, e.g., replace $\forall r. \top$ with \top [19]. However this treatments result in increasing runtime requirements. Arguably, using such heuristic functions, handcrafted rules or reasoners hinders tackling CEL problem in large setting due to increased memory or runtime requirements.

In this work, we regard the problem of finding a hypothesis $H \in \mathcal{H}$ as a sequential decision-making problem and formalize it within the setting of Reinforcement Learning (RL). Therein, state-of-the-art CEL approaches are analogous to myopic RL agents as their objectives are set to solely maximize immediate rewards (see Section 5). In contrast, deep RL is designed to address the problem of learning how to incorporate consideration for future states in immediate actions [34,26]. Thus, we propose a convolution deep Q-learning model (dubbed DRILL) to efficiently steer the search towards \mathcal{H} , while incorporating consideration for future states in immediate decisions. Hence, the problem of finding a hypothesis is formalized as training DRILL to select actions in a fashion that maximizes *cumulative discounted future rewards*.

To train DRILL, we adapt the idea of playing Atari 2600 games and design an unsupervised training procedure in a fashion akin to [26]. Our approach to training ensures that DRILL can be trained on KGs with no adjustment of the architecture. For a given learning problem, we first construct a quasi-ordered state space as a RL environment, where each RL state is represented with continuous vector representations (*embeddings*) of individuals belonging to the respective

OWL class expression. Next, DRILL begins to interact with this environment by refining the most general state $\rho(\top)$. Subsequently, DRILL selects next possible states $s_i \in \rho(\top)$ via ϵ -greedy fashion (see Section 5). Thereupon, DRILL receives the reward for transitioning from s_i to the next state s_j that it selects.

Our experiments are carried out on the description logic \mathcal{ALC} and show that DRILL is able to steer the search for elements of \mathcal{H} more efficiently than state-of-the-art approaches. DRILL finds goal states **at least 2.7 times faster** than state-of-the-art approaches on benchmark datasets. Importantly, DRILL is able to estimate heuristic values of more than 10^3 states in a second on standard hardware. The main contributions of this paper are threefold:

1. We model CEL using refinement operators within the framework of RL.
2. We present a convolutional model for predicting the cumulative discounted future reward for states within an infinite state space.
3. We provide an open-source implementation of our framework to foster research in the direction of combining reinforcement learning with class expression learning.

2 Related Work

Our work is grounded in two areas of research, i.e., CEL and RL. One of the first works of supervised learning in description logic is presented in [7]. Later, Badea et al. [1] propose to apply a refinement operator in a top-down fashion. YINYANG [18] effectively combines the previous approaches to learn class expressions. OCEL [19], ELTL and CELOE [20] use a proper and complete refinement operator to build a search tree of OWL class expressions. Therein, each node corresponds to an OWL class expression and is annotated with a respective heuristic and quality values. In Section 3.1, we elucidate the working of OCEL, ELTL and CELOE. In turn, DL-FOIL [14] proposes to use unlabeled individuals in its heuristic function to take the open world assumption into account.

Over the past decade, there have been a number of successes in learning policies for sequential decision-making problems. Notable examples include deep Q-learning for Atari game-playing [26] and strategic policies joined with search led to defeating a human expert at the game of Go [33]. Likewise, various RL models have been applied in diverse tasks on KGs, including question answering, link prediction, fact checking and knowledge graph completion [38,35,8,24,36].

3 Preliminaries

3.1 Class Expression Learning in Description Logics

We define the problem of class expression learning in a fashion akin to [20,19,23,21]. Given a $\mathcal{G} = (Tbox, Abox)$, a set of positive E^+ and negative examples E^- as well as a formal logic \mathcal{L} (e.g., \mathcal{ALC}), the goal is to find a class expression $H \in \mathcal{H}$ defined as

$$\forall H \in \mathcal{H} : \{(\mathcal{G} \models H(p)) \wedge (\mathcal{G} \models \neg H(n))\} \text{ s.t. } \forall p \in E^+, \forall n \in E^-. \quad (1)$$

The problem of finding hypotheses is transformed into a search problem within a quasi-ordered state space (\mathcal{S}, \preceq) [20], where each state corresponds to a class expression. A quasi-ordering imposes a reflexive and transitive relation between states. The quality of a given class expression is often determined by means of accuracy or F1-measure [20]. Traversing in \mathcal{S} is commonly conducted via top-down refinement operators $\rho : \mathcal{S} \rightarrow 2^{\mathcal{S}}$ [22]:

$$\forall s_i \in \mathcal{S} : \rho(s_i) \subseteq \{s_j \in \mathcal{S} \mid s_j \preceq s_i\}, \quad (2)$$

where $\rho(s_i)$ yields a set of *specialisations* of s_i . The search tree is initialized via adding the most general state (\top) as a root node. The initialized search tree is iteratively built by selecting a node containing the most promising state and adding its qualifying refinements as its children into a search tree. Figure 1 illustrates an excerpt of traversing \mathcal{S} and building a search tree for a learning problem on a fictitious university ontology.

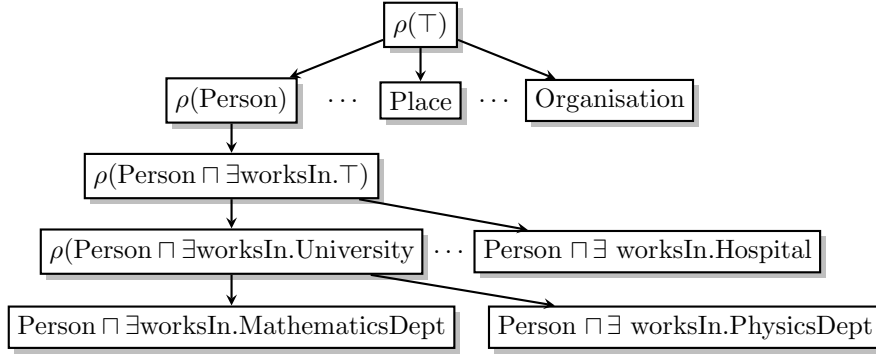


Fig. 1. Illustration of traversing \mathcal{S} and building a search tree in \mathcal{ACC}

3.2 Heuristic functions

A major challenging part of this search problem is to find a suitable heuristic function that efficiently steers the search towards elements of \mathcal{H} [20]. A heuristic function quantifies how adequately a class expression fits a learning problem and guides the search in a learning process [20].

To introduce heuristic functions of state-of-the-art approaches, we first define the retrieval function. Let C, I be all class expressions in \mathcal{L} and all individuals in $Abox$, respectively. We follow Definition 2.17 in [19] and define the retrieval function as $\mathcal{R} : C \mapsto I$. \mathcal{R} maps class expressions to the set of its instances, e.g. $\mathcal{R}(\mathbf{Person})$ will contain all instances of the class **Person**. The heuristic of OCEL is defined as

$$\phi_{\text{OCEL}}(c_i, c_j) = A(c_j) + \lambda \cdot [A(c_j) - A(c_i)] - \beta \cdot z, \quad (3)$$

where $\beta > \lambda \geq 0$ and $z \in \mathbb{N}$ stands for the horizontal expansion value [19] and A is defined as

$$A(c) = 1 - \frac{|E^+ \setminus \mathcal{R}(c)| + |\mathcal{R}(c) \cap E^-|}{|E^+| + |E^-|}. \quad (4)$$

$A(c_i)$ quantifies the quality of a class expression c_i w.r.t. E^+ and E^- , whereas $\phi_{\text{OCEL}}(c_i, c_j)$ determines the heuristic value of c_j given c_i w.r.t. E^+ and E^- . ELTL replaces the stepwise horizontal expansion technique used in OCEL with a penalty for the length of a concept. CELOE extends OCEL and ELTL by redefining the accuracy of a class expression and replacing z with a length bias (see the definition 5.4 in [19]) to incorporate the number of all individuals in the computation of heuristic values. The heuristic function of CELOE is defined as

$$\phi_{\text{CELOE}}(c_i, c_j) = A(c_j) + \lambda \cdot [A(c_j) - A(c_i)] - \beta \cdot |c_j|, \text{ where} \quad (5)$$

$$A(c, t) = 1 - 2 \cdot \frac{t \cdot |E^+ \setminus \mathcal{R}(c)| + |\mathcal{R}(c) \setminus E^+|}{(t+1) \cdot |I|}. \quad (6)$$

$t > 1$ and $|c_j|$ is the length of c_j . Note that for the sake of brevity, we do not introduce a new symbol for a node containing a class expression with a score and horizontal expansion in Equation (3) and Equation (5).

3.3 Reinforcement Learning

In RL, a Markov Decision Process (MDP) is applied to model the synchronous interaction between an *agent* and an *environment*. An MDP is defined by a 5-tuple $\langle \mathbf{S}, \mathbf{A}, \mathbf{R}, \mathbf{T}, \gamma \rangle$, which comprises of a set of states \mathbf{S} , a set of actions \mathbf{A} , a reward function \mathbf{R} , a transition function \mathbf{T} and the discount rate $\gamma \in [0, 1)$. Given a state $\mathbf{s}_t \in \mathbf{S}$ at time t , an agent carries out an action $\mathbf{a}_t \in \mathbf{A}(\mathbf{s}_t)$ from a set of available actions on \mathbf{s}_t . Upon taking action, the agent receives a reward R_{t+1} and reaches the next state \mathbf{s}_{t+1} . Hence, R_{t+1} corresponds to the reward of taking action \mathbf{a}_t on \mathbf{s}_t and reaching \mathbf{s}_{t+1} .² The probability of reaching \mathbf{s}_{t+1} and receiving R_{t+1} by taking action \mathbf{a}_t in a given \mathbf{s}_t assigned by \mathbf{T} . This synchronous interaction between an agent and environment induces a *trajectory*. A trajectory is a sequence of states, actions and rewards. The *discounted return* of the t^{th} item in a trajectory is defined as

$$G_t = R_{t+1} + \gamma R_{t+2} + \gamma^2 R_{t+3} + \dots = \sum_{k=0} \gamma^k R_{t+k+1}, \quad (7)$$

where the discount rate $0 \leq \gamma < 1$ determines the present value of future rewards. The goal of an RL agent is to select actions in a fashion that maximizes the discounted return [34].

² We follow the terminology used in [34].

Acting optimally. A policy π prescribes which action to take in a given state. An optimal policy π^* hence prescribes optimal actions on any states so that G_t is maximized. To obtain π^* , value functions are often used. Let $V_\pi : \mathbf{S} \mapsto \mathbb{R}$ be the state-value function for a policy π . $V_\pi(\mathbf{s})$ is defined as

$$V_\pi(\mathbf{s}) = \mathbb{E}_\pi [G_t \mid \mathbf{s}_t = \mathbf{s}], \quad (8)$$

$$= \mathbb{E}_\pi [R_{t+1} + \gamma G_{t+1} \mid \mathbf{s}_t = \mathbf{s}] \quad (9)$$

$$= \mathbb{E}_\pi \left[\sum_{k=0}^{\infty} \gamma^k R_{t+k+1} \mid \mathbf{s}_t = \mathbf{s} \right], \quad (10)$$

where $\mathbb{E}_\pi [\cdot]$ stands for the expected value of a random variable given that π is followed. Similarly, The action-value function $Q_\pi : \mathbf{S} \times \mathbf{A} \mapsto \mathbb{R}$ of a policy π for a state \mathbf{s} and an action \mathbf{a} is defined as

$$Q_\pi(\mathbf{s}, \mathbf{a}) = \mathbb{E}_\pi [G_t \mid \mathbf{s}_t = \mathbf{s}, \mathbf{a}_t = \mathbf{a}], \quad (11)$$

$$= \mathbb{E}_\pi [R_{t+1} + \gamma G_{t+1} \mid \mathbf{s}_t = \mathbf{s}, \mathbf{a}_t = \mathbf{a}] \quad (12)$$

$$= \mathbb{E}_\pi \left[\sum_{k=0}^{\infty} \gamma^k R_{t+k+1} \mid \mathbf{s}_t = \mathbf{s}, \mathbf{a}_t = \mathbf{a} \right]. \quad (13)$$

Using the Bellman equation, optimal value functions can be obtained recursively:

$$V_*(\mathbf{s}) = \max_{\mathbf{a} \in \mathbf{A}(\mathbf{s})} \mathbb{E} [R_{t+1} + \gamma V_*(\mathbf{s}_{t+1}) \mid \mathbf{s}_t = \mathbf{s}, \mathbf{a}_t = \mathbf{a}]; \quad (14)$$

$$Q_*(\mathbf{s}, \mathbf{a}) = \mathbb{E} \left[R_{t+1} + \gamma \max_{\mathbf{a}' \in \mathbf{A}(\mathbf{s}_{t+1})} Q_*(\mathbf{s}_{t+1}, \mathbf{a}') \mid \mathbf{s}_t = \mathbf{s}, \mathbf{a}_t = \mathbf{a} \right]. \quad (15)$$

Equation (15) establishes the relationship between the optimal value of a state-action pair and its successor state-action pairs [34]. An optimal policy π_* can be readily obtained if Q_* is known, since any policy that is greedy with respect to Q_* is optimal.³

Learning to act optimally. Q_* can be approximated by using the iterative Q-learning update:

$$Q_{i+1}(\mathbf{s}_t, \mathbf{a}_t) \leftarrow Q_i(\mathbf{s}_t, \mathbf{a}_t) + \alpha [R_{t+1} + \gamma \max_{\mathbf{a} \in \mathbf{A}(\mathbf{s}_{t+1})} Q_i(\mathbf{s}_{t+1}, \mathbf{a}) - Q_i(\mathbf{s}_t, \mathbf{a}_t)], \quad (16)$$

where the learning rate is denoted with $\alpha \in (0, 1]$. Through using the iterative update defined in Equation (16), Q_i converges to Q_* as $i \rightarrow \infty$ [34]. However, iteratively approximating exact optimal values is often computationally infeasible. For instance, solving the Bellman equation for Q_* for the game of backgammon (with about 10^{20} states) would require years of computation even on currently available computers [34]. In practice, a neural network parameterized with Θ (known as a Q-network) is commonly applied to estimate the optimal action-value function, $Q(s, a; \Theta) \approx Q_*(s, a)$ [26]. This approach is known as deep Q-learning and allows to effectively apply reinforcement learning even in problems with large state-action spaces [34, 26].

³ We refer Section 3.8 in [34] for the derivation of Q_* by using the Bellman equation.

4 Refinement Operator

Let N_C be a set of finite named concepts and let R be a finite set of roles. We write \top to denote the top concept and \perp to denote the bottom concept. We set $N_C^+ = N_C \cup \{\top, \perp\}$. We define S to be the set of all \mathcal{ALC} concepts built upon N_C and R . Formally this the following:

- $N_C^+ \subset S$;
- If $C \in S$ and $D \in S$, then $(C \sqcap D) \in S$
- If $C \in S$ and $D \in S$, then $(C \sqcup D) \in S$
- If $C \in S$ and $r \in R$, then $\exists r.C \in S$
- If $C \in S$ and $r \in R$, then $\forall r.C \in S$
- If $C \in S$ then $(\neg C) \in S$

Let $X, Y \in S$ and $r \in R$. We define the length of a concept $C \in S$ (denoted $|C|$) as follows:

- If $C \in N_C^+$, then $|C| = 1$;
- If $C = X \sqcup Y$ or $C = X \sqcap Y$, then $|C| = |X| + |Y| + 1$;
- If $C = \exists r.X$ or $C = \forall r.X$, then $|C| = |X| + 2$;
- If $C = \neg X$, then $|C| = |X| + 1$.

The length of a concept is an ordering over the set S . We define the operator ρ over $(S, |\cdot|)$ as follows:

$$\rho(C) = \begin{cases} \{\exists r.C, \forall r.C, C \sqcap \top, C \sqcup \top, \neg C, C\} & \text{for any } C \\ \{\exists r.\rho(X)\} & \text{if } C = \exists r.X \\ \{\forall r.\rho(X)\} & \text{if } C = \forall r.X \\ \{\neg\rho(X)\} & \text{if } C = \neg X \\ \{\rho(X) \sqcup \rho(Y)\} & \text{if } C = X \sqcup Y \\ \{\rho(X) \sqcap \rho(Y)\} & \text{if } C = X \sqcap Y \\ N_C^+ & \text{if } C = \top \end{cases} \quad (17)$$

In the following, we will assume that ρ begins the refinement process from \top .

Theorem 1. ρ is an upward refinement operator over $(S, |\cdot|)$

Proof. We need to prove that $|\rho(C)| \geq |C|$. This is a direct consequence of the construction of C . For each possible refinement computed ρ and by virtue of the definition of $|\cdot|$, it is easy to see that ρ either preserves the length of a concept (e.g., if $C \in N_C^+$) or leads to longer concepts (e.g., for some refinements in the first line of the specification of C). \square

In the following, we will use the following convention: the operator ρ^* will stand for the transitive closure of ρ . Ergo, if D can be generated from C by ρ through manifold application, we will simply write $D \in \rho(C)$.

Every \mathcal{ALC} concept C can be represented as a tree. This is a direct consequence of the definition of \mathcal{ALC} concepts. For example, all concepts $C \in N_C^+$

can be represented by trees with exactly one node and not edges. If $C \notin N_C^+$, then C can only take one of five forms:

Two observations are important here. First, there can be several tree representations for any concept C . We define the height $h(C)$ by choosing the smallest height h_{\min} over all possible tree representations of C and setting the height of C , denoted $h(C)$, to exactly h_{\min} .

The second observation is that only elements of N_C^+ have height 0, which is a direct consequence of the construction of complex concepts in \mathcal{ALCC} : If the concept $C \notin N_C^+$, then it must have a length of at least 2 as its tree representation must hence contain at least 2 nodes. By virtue of the definition of the height of a tree, a tree with two nodes must have a height of at least 1.

Lemma 1. *ρ can generate any concept of height 0.*

Proof. Note that only elements of N_C^+ have height 0. By virtue of the last line of its specification, ρ can generate all elements of N_C^+ and thus all elements of height 0. \square

Lemma 2. *Assume $n \geq 0$. If ρ can generate all concepts with a height $h \leq n$, then it can generate all concepts of height $n + 1$.*

Proof. A concept C of height $n + 1$ can be written in one of five ways:

1. $C = \exists r.X$
2. $C = \forall r.X$
3. $C = \neg X$
4. $C = X \sqcup Y$
5. $C = X \sqcap Y$

Let us begin by considering the first three possibilities. By definition of the height, $h(C) > h(X)$. Hence, by virtue of our assumption, ρ can generate X . Now the first generation rule of ρ states that $\exists r.X$, $\forall r.X$ and $\neg X$ belong to the possible refinements of X . Hence, ρ can generate C for these three cases.

We are left with two possibilities: $C = X \sqcup Y$ or $C = X \sqcap Y$. In both cases, we can assume that $|X| \geq |Y|$ without loss of generality. We prove that ρ can generate $C = X \sqcap Y$. The other possibility can be addressed analogously. By the definition of height of a tree, $h(X) = n$. If it were not the case, then $h(Y) < n$ would also hold, leading to $h(X) < n + 1$, which would contradict the assumption on the height of X made in the premise of this proof. Now, given that $h(X) = n$, it can be generated by ρ by virtue of the assumption of this lemma. Similarly, $h(Y) \leq n$ also means that it can be generated by ρ by virtue of the assumption of this lemma. Remember that all concepts are generated from \top . We can now show that there must be a refinement path that leads to C . First, given that ρ can generate X , there is a refinement path from \top to X , i.e., $X \in \rho^*(\top)$. Consequently, $(X \sqcap \top) \in \rho^*(\top)$ by virtue of the first rule in the specification of ρ . $\rho(X \sqcap \top) = \rho(X) \sqcap \rho(\top)$. As $X \in \rho(X)$, we solely need to show that $Y \in \rho(\top)$. This is a direct consequence of $h(Y) \leq n$ as we assumed that every concept of height n can be generated by ρ and every concept that can be generated by ρ is an element of $\rho^*(\top)$. \square

Theorem 2. *Given a set of named concepts N_C , ρ can generate all \mathcal{ALC} concepts based on N_C .*

Proof. This is a direct consequence of the two lemmas above.

It is obvious that ρ is *redundant*, i.e., there can be more than one sequence of refinement from \top to a concept C . The operator is *finite* as $|\rho(C)| < \infty$ for any \mathcal{ALC} concepts C built upon a finite set of named concepts N_C and a finite set of roles. We mostly exploit these two characteristics during the implementation of the refinement operator.

5 Methodology

Intuition. Devising a suitable heuristic function is crucial in CEL [20]. The search of \mathcal{H} is steered by optimizing a heuristic $\phi : \mathcal{S} \times \mathcal{S} \mapsto \mathbb{R}$ signals whether refining the input state assists to find $H \in \mathcal{H}$ as elucidated in Section 3.1. Equations (3) and (5) show that state-of-the-art CEL models rely on heuristic functions that determine promises without any consideration for future states. More specifically, $\phi(s_i, s_j)$ is computed without incorporating any information pertaining to $\{s_k \mid s_k \in \mathcal{S} \wedge s_k \preceq s_j\}$. In the RL framework, this is analogous to setting $\gamma = 0$ in Equation (7), i.e., to setting the present value of future rewards to 0. This implies that heuristic functions of state-of-the-art CEL models correspond to **myopic policies**, whose only concern is to maximize immediate rewards (see Section 3.3 in [34], or Section 3 in [6]). Playing a chess under a myopic policy corresponds to ignoring any future configurations of the board while selecting one’s move.

We leverage the deep Q-learning framework to incorporate information pertaining to $\{s_k \mid s_k \in \mathcal{S} \wedge s_k \preceq s_j\}$ while determining the heuristic value of the transition from a state s_j to a state s_i . We represent RL states \mathbf{s}_i by means of a vector in $\mathbb{R}^{|\mathcal{R}(c_i)| \times d}$ obtained by embedding the elements of $\mathcal{R}(c_i)$ in \mathbb{R}^d . Ergo, the root RL state \mathbf{s}_\top captures all relevant information pertaining to any states by means of embeddings of $\mathcal{R}(\top)$. Taking an action \mathbf{a}_j on \mathbf{s}_i implies refining s_i in the refinement tree and reaching a state s_j . Upon taking an action \mathbf{a}_j , DRILL deterministically reaches a RL state \mathbf{s}_j and receives a reward, i.e., $\mathbb{P}(\mathbf{s}_j, \mathbf{r} \mid \mathbf{s}_i, \mathbf{a}_j) = 1$.

The number of possible actions $|\mathbf{A}(\mathbf{s}_i)|$ on a given RL state \mathbf{s}_i corresponds to $|\rho(s_i)|$. Hence, the number of actions per state is not fixed in this environment. This entails that the standard deep Q-network loss function can not be directly applied [26]. To mitigate this issue, we adapt the state-state value function $Q(\mathbf{s}_i, \mathbf{s}_j)$. Edwards et al. [13] showed that the state-state Q function naturally *avoid redundant actions*. As the number of redundant actions increases, using the state-state Q function results in more favorable results than using the state-action Q function. With these considerations, we define the following loss

function

$$\mathcal{L}(\Theta) = \mathbb{E}_{\mathbf{s}_i, \mathbf{s}_j, \mathbf{e}_+, \mathbf{e}_- \sim \mathcal{D}} \left[\left(\mathbf{r} + \gamma \max_{\mathbf{s}_x \preceq \mathbf{s}_k} Q(\mathbf{s}_k, \mathbf{s}_x \mid \mathbf{e}_+, \mathbf{e}_-) - \phi_{\text{DRILL}}(\mathbf{s}_i, \mathbf{s}_j, \mathbf{e}_+, \mathbf{e}_-) \right)^2 \right]. \quad (18)$$

$\theta, e_+, e_-, \mathbf{r}, \mathcal{D}$ and $\max_{\mathbf{s}_x \preceq \mathbf{s}_k} Q(\mathbf{s}_k, \mathbf{s}_x \mid \mathbf{e}_+, \mathbf{e}_-)$ denote parameters of DRILL, embeddings of E^+ , E^- , the experience replay, a reward of reaching \mathbf{s}_j from \mathbf{s}_i w.r.t. E^+ and E^- , and a maximum reachable Q-value from \mathbf{s}_j , respectively.

Approach. To minimize Equation (18), we propose DRILL—a fully connected convolutional network parameterized with $\Theta = [\omega, \mathbf{W}, \mathbf{H}, \mathbf{b}_1, \mathbf{b}_2]$. More specifically, DRILL is defined as

$$\phi_{\text{DRILL}}(\mathbf{x}) = f \left(\text{vec}(f[\Psi(\mathbf{x}) * \omega]) \cdot \mathbf{W} + \mathbf{b}_1 \right) \cdot \mathbf{H} + \mathbf{b}_2, \quad (19)$$

where \mathbf{x} represents $[\mathbf{s}_i, \mathbf{s}_j, \mathbf{e}_+, \mathbf{e}_-]$: $\mathbf{s}_i \in \mathbb{R}^{|\mathcal{R}(c_i)| \times d}$, $\mathbf{s}_j \in \mathbb{R}^{|\mathcal{R}(c_j)| \times d}$, $\mathbf{e}_+ \in \mathbb{R}^{|E^+| \times d}$, and $\mathbf{e}_- \in \mathbb{R}^{|E^-| \times d}$. $\Psi(\cdot)$ converts \mathbf{x} into $\mathbb{R}^{4 \times d}$ by averaging the embeddings of its input. Hence, cumulated discounted future rewards are determined by considering the centroid of embeddings.⁴ Moreover, $f(\cdot)$, $\text{vec}(\cdot)$, $*$ and ω correspond the rectified linear unit function (ReLU), a flattening operation, the convolution operation, and kernels in the convolution operation. Two consecutive affine transformations are denoted with $(\mathbf{W}, \mathbf{b}_1)$ and $(\mathbf{H}, \mathbf{b}_2)$, respectively.

To train DRILL, we designed an unsupervised training scenario to automatically create learning problems in a fashion akin to [26].

5.1 Unsupervised Training

Learning Problem Generation. We first randomly generate n goal states. To this end, we iteratively apply ρ in a randomized depth-first search manner starting from \top , i.e., our random state generator select the next state to refine by randomly selecting states and refining them starting from $\rho(\top)$. During this process, states s that satisfy the length constraint $\{s \mid 1 \leq |s| \leq \text{maxlen}\}$ are stored. Initially, we set $\text{maxlen} = 5$. To avoid storing similar states, we performed this task m times. Consequently, we obtain at most $n \times m$ states. For each stored state, we compute all positive and negative examples, i.e., $E^+ = \mathcal{R}(c)$ and $E^- = I \setminus \mathcal{R}(c)$, respectively. This operation often results in creating imbalanced E^+ and E^- , with $|E^-| \gg |E^+|$ being common. To alleviate imbalanced examples, we randomly undersample the largest set of examples so that $|E^+| = |E^-|$ and repeat this process κ times. Consequently, we generated at most $n \times m \times \kappa$ learning problems. During the learning problem generation, we also considered introducing a size constraint at learning problem generation, $\{c \mid 1 \leq |c| \leq \text{maxlen} \wedge .1|I| \leq |\mathcal{R}(c)| \leq .3|I|\}$.

⁴ This is clearly not the only viable approach to achieve this goal. In future, we plan to use LSTM and Transformer architectures instead of averaging embeddings.

Training Procedure. Algorithm 1 elucidates the training procedure. We design this procedure in a fashion akin to [26]. For the sake of brevity, we used \mathbf{s}_i to denote the vector representation of embeddings of c_i and its counterpart s_i in the refinement tree. Algorithm 1 explicitly shows that at 15th line, a target max. Q-value y_i corresponds to the sum of an immediate reward \mathbf{r}_i and maximum Q-value obtained on remaining transactions $\mathcal{T}[i:]$.

Algorithm 1 DRILL with deep Q-learning training procedure

- 1: **Require:** Replay memory \mathcal{D} , # of episodes M , # of actions T , update constant U , reward function \mathbf{R} and refinement operator ρ
 - 2: Initialize Θ with Glorot initialization
 - 3: **for** $m = 1, M$ **do** ▷ Sequence of Episodes
 - 4: Initialise the search process $\mathbf{s}_0 = \top$ and the transition storage \mathcal{T}
 - 5: **for** $i = 0, T$ **do** ▷ Sequence of Actions
 - 6: Refine the current state $\rho(\mathbf{s}_i)$
 - 7: Select a random state $\mathbf{s}_j \in \rho(\mathbf{s}_i)$ with probability ϵ
 - 8: otherwise select $\mathbf{s}_j = \max_{\mathbf{s}_j \in \rho(\mathbf{s}_i)} \phi_{\text{DRILL}}([\mathbf{s}_i, \mathbf{s}_j, \mathbf{e}_+, \mathbf{e}_-]); \Theta)$
 - 9: Compute reward $\mathbf{r}_i = \mathbf{R}(\mathbf{s}_i, \mathbf{s}_j)$
 - 10: Store transition $\mathcal{T}[i] = [\mathbf{s}_i, \mathbf{s}_j, \mathbf{e}_+, \mathbf{e}_-, \mathbf{r}_i]$
 - 11: Set $\mathbf{s}_{i+1} = \mathbf{s}_j$
 - 12: Reduce ϵ with a constant ▷ Reduction of Exploration
 - 13: **for** $i = 0, T$ **do** ▷ Target Q-values
 - 14: Select transition $[\mathbf{s}_i, \mathbf{s}_j, \mathbf{e}_+, \mathbf{e}_-, \mathbf{r}_i] = \mathcal{T}[i]$
 - 15: Compute target value y_i in $\mathcal{T}[i:]$ according to Equation (7)
 - 16: Store $(\mathbf{s}_i, \mathbf{s}_j, \mathbf{e}_+, \mathbf{e}_-, y_i)$ in \mathcal{D}
 - 17: **if** $m \% U == 0$ **then** ▷ Updating Parameters
 - 18: Sample random minibatches from \mathcal{D}
 - 19: Compute loss of minibatches w.r.t. Equation (18)
 - 20: Update Θ accordingly
-

Construction of Rewards and Connection to CELOE. To compute rewards, we rely on ϕ_{CELOE} and defined the reward function as

$$\mathbf{R}(\mathbf{s}_i, \mathbf{s}_j) = \begin{cases} \text{maxreward}, & \text{if F1-measure}(c_j) = 1. \\ \phi_{\text{CELOE}}(c_i, c_j), & \text{otherwise.} \end{cases} \quad (20)$$

Equation (20) shows that DRILL is expected to steer the search towards shorter class expressions as ϕ_{CELOE} favors shorter class expressions (see Equation (5)).

6 Experiments

6.1 Datasets

We used four benchmark datasets (Family, Carcinogenesis, Mutagenesis and Biopax) to evaluate DRILL [23,2,14,15]. An overview of the datasets is provided in Table 1. We refer [2,15] for details pertaining to benchmark datasets.

Table 1. Overview of benchmark datasets.

Dataset	#instances	#concepts	#obj. properties	#data properties	DL language
Family	202	18	4	0	\mathcal{ALC}
Carcinogenesis	22372	142	4	15	$\mathcal{ALC}(\mathcal{D})$
Mutagenesis	14145	86	5	6	$\mathcal{AL}(\mathcal{D})$
Biopax	323	28	19	30	$\mathcal{ALCHF}(\mathcal{D})$

6.2 Experimental Setup

We based our experimental setup on [4]. Hence, we evaluated DRILL by using the learning problems provided therein. In our experiments, we evaluate DRILL in \mathcal{ALC} for CEL. However, DRILL can be ported to all Description Logics. All experiments were carried out on Ubuntu 18.04 with 16 GB RAM with Intel(R) Core(TM) i5-7300U CPU v4 @ 2.60GHz.

Training. To train DRILL, we first generate 10 learning problems for each benchmark datasets described in Section 5.1. During our experiments, we used the pretrained embeddings of input knowledge graphs provided by [10,9]. We used ConEx embeddings of Family, Biopax, Mutagenesis and Shallop embeddings of Carcinogenesis. For more details about configurations of models, we refer project pages of [10,9]. For each generated learning problem, we trained DRILL in an ϵ -greedy fashion by using the the following configuration: ADAM optimizer with learning rate of .01, mini-batches of size 512, number of episodes set to 100, an epsilon decay of .01, a discounting factor γ of .99, 32 input channels, and (3×3) kernels. The parameter selection was carried out based on [10,26]. The offline training on all benchmark datasets took 21 minutes on Biopax, 18 minutes on Family, 143 minutes on Mutagenesis and 119 on Carcinogenesis. Note that the offline training time is not relevant for the evaluation of CEL as CEL occurs online.

Learning Problem Generation. To perform an extensive comparison between approaches, we automatically generate learning problems by using the procedure defined in Section 5.1. During our evaluation, we ensured that the set of learning problems used during training for DRILL did not overlap with the set of learning problems used for evaluation.

Stopping Criteria. We used two standard stopping criteria for approaches. (i) We set the maximum runtime to 3 seconds as Lehmann et al. [23] showed that models often reach good solutions within 1.5 seconds. (ii) Approaches were configured to terminate if a goal state found.

Evaluation Metrics. We compared approaches via F1-score, accuracy, the runtime and number of tested class expressions as similarly done in [23]. The F1-score and accuracy were used to measure the quality of the class expressions found w.r.t. positive and negative examples, while the runtime and the number of tested class expressions were used to measure the efficiency.

Implementation Details and Reproducibility. To ensure reproducibility of our results, We provide an open-source implementation of our approach, including training and evaluation scripts as well as pretrained models.⁵

7 Results

Table 2 reports results on standard learning problems provided within the DL-Learner framework [4]. These results suggest that approaches yield similar performances in terms of F1-score and accuracy on benchmark datasets. However, DRILL outperforms all other approaches on all datasets w.r.t. its runtime. On all benchmark datasets, DRILL requires at most **4 seconds** to yield competitive performance, while CELOE and ELTL require at most **21 seconds** and **18 seconds**, respectively. Hence, DRILL is at least **2.7 times** more time-efficient than CELOE, OCEL and ELTL on all standard learning problems. During our experiments, we observed that (1) the number of tested class expressions in ELTL and (2) the F1-score of the best found class expression in OCEL are not reported.

Table 2 indicates that CELOE explores less number of states than other approaches. This may stem from (1) redundancy elimination and (2) expression simplification. (1) entails to query whether an expression already exists in the search tree. If yes, then this expression is not added into the search tree (see section 6.1 in [22]). (2) reduces long expressions into shorter ones, e.g., $\top \sqcup \text{Person}$ and $\forall r. \top$ into **Person** and \top , respectively. These modifications often lead to explore less number of states, i.e. reduce the memory requirement. However, they often introduce extra computations, i.e., increase runtime.

Note that we also evaluated DL-FOIL in our initial experiments. However, we observed that DL-FOIL often failed to terminate within 5 minutes. This may stem from the fact: (i) DL-FOIL does not use the elapsed time as a stopping criterion (see Section 4 [14]). (ii) DL-FOIL requires to find an expression not involving E^- to terminate (see Figure 1 in [14]). Consequently, we could not include DL-FOIL in our experiments.

Table 3 show the details of our evaluation on 18 learning problems on the Family dataset in detail. These details suggest that DRILL and CELOE often

⁵ <https://github.com/dice-group/DRILL>

Table 2. Results on benchmark datasets. F1, Acc, T and Exp. denote the length of predicted class expression, the F1-score, the accuracy, runtime in seconds, and number of class expression tested respectively. † stands for no solution found and by the respective approach. * indicates that respective value is not reported in DL-Learner.

Dataset	Drill				CELOE				OCEL				ELTL			
	F1	Acc.	T	Exp.	F1	Acc.	T	Exp.	F1	Acc.	T	Exp.	F1	Acc.	T	Exp.
Family	0.960	0.950	1.23	2168	0.970	0.970	3.63	646	*	.940	6.12	2756	.960	.950	3.39	*
Carcinogenesis	0.710	0.560	4.23	305	0.710	0.560	21.14	230	†	†	23.49	802	.710	.570	22.14	*
Mutagenesis	0.700	0.540	3.04	3941	0.700	0.540	13.90	135	†	†	13.21	4023	.700	.540	13.21	*

Table 3. Results of single learning problems on the Family benchmark dataset. † stands for no solution found by the respective approach. L, F1, Acc and T denote the length of predicted class expression, the F1-score of prediction, the accuracy of prediction and runtime in seconds, respectively.

Expression	Drill				CELOE				OCEL				ELTL			
	L	F1	Acc	T	L	F1	Acc	T	L	F1	Acc	T	L	F1	Acc	T
Aunt	6	0.83	0.79	3.3	6	0.83	0.79	5.7	16	*	1.00	5.8	1	.800	0.76	2.8
Brother	1	1.00	1.00	0.2	1	1.00	1.00	2.9	1	*	1.00	5.8	5	1.00	1.00	3.8
Cousin	4	0.73	0.65	2.9	5	0.79	0.74	5.9	21	*	1.00	6.2	1	0.66	0.50	3.0
Daughter	1	1.00	1.00	0.2	1	1.00	1.00	2.9	1	*	1.00	5.9	3	1.00	1.00	2.9
Father	1	1.00	1.00	0.2	1	1.00	1.00	3.0	1	*	1.00	6.0	3	1.00	1.00	3.0
Granddaughter	1	1.00	1.00	0.2	1	1.00	1.00	3.1	1	*	1.00	5.3	1	1.00	1.00	2.9
Grandfather	1	1.00	1.00	0.2	1	1.00	1.00	2.9	1	*	1.00	5.7	1	1.00	1.00	3.0
Grandgranddaughter	1	1.00	1.00	0.2	1	1.00	1.00	2.9	1	*	1.00	5.9	7	1.00	1.00	3.01
Grandgrandfather	1	0.94	0.94	3.2	5	1.00	1.00	3.0	5	*	1.00	5.8	7	1.00	1.00	3.7
Grandgrandmother	9	0.94	0.94	3.3	5	1.00	1.00	3.1	5	*	1.00	5.9	7	1.00	1.00	3.7
Grandgrandson	1	0.92	0.92	3.5	5	1.00	1.00	5.7	5	*	1.00	6.6	7	1.00	1.00	3.1
Grandmother	1	1.00	1.00	0.2	1	1.00	1.00	2.8	1	*	1.00	5.9	1	1.00	1.00	3.1
Grandson	1	1.00	1.00	0.2	1	1.00	1.00	2.8	1	*	1.00	6.0	1	1.00	1.00	3.0
Mother	1	1.00	1.00	0.2	1	1.00	1.00	2.9	1	*	1.00	5.9	5	1.00	1.00	3.1
PersonWithASibling	1	1.00	1.00	0.2	1	1.00	1.00	2.8	1	*	1.00	7.0	1	1.00	1.00	3.1
Sister	1	1.00	1.00	0.2	1	1.00	1.00	2.8	1	*	1.00	5.8	5	1.00	1.00	3.0
Son	1	1.00	1.00	0.2	1	1.00	1.00	3.0	1	*	1.00	5.7	3	1.00	1.00	2.9
Uncle	6	0.90	0.89	2.9	6	0.90	0.89	5.9	†	†	†	5.8	1	0.88	0.87	2.9

converge towards shorter concepts compared to OCEL and ELTL. This may stem from the fact that DRILL indeed learned to assign low values for longer concepts as DRILL is trained on rewards based on the heuristic function of CELOE. DRILL finds a goal state within a second in 12 out of 18 learning problems. During our experiments, we observed that approaches implemented in the DL-Learner framework do not terminate within the set maximum runtime. We delved into their implementations in the DL-Learner framework and observed that the maximum runtime criterion is not checked until refinements of a given class expression are obtained. During our experiments, we observed that there are only few learning problems per dataset. To perform more extensive comparisons between approaches, we automatically and randomly generate more learning problems. Table 4 reports results on 370 learning problems gen-

erated automatically on benchmark datasets. These results confirm that DRILL finds a goal state faster than all other approaches, while CELOE explores fewer expressions than all other approaches.

Table 4. Results on automatically generated learning problems on four benchmark datasets. #LP stands for the number learning problems.

Dataset	#LP	Drill				CELOE				OCEL				ELTL			
		F1	Acc.	T	Exp	F1	Acc.	T	Exp	F1	Acc.	T	Exp	F1	Acc.	T	Exp
Family	74	1.00	1.00	1.1	32.2	1.00	1.00	3.6	14.2	*	1.00	6.20	2403.0	1.00	1.00	3.52	*
Carcinogenesis	100	1.00	1.00	2.2	47.5	1.00	1.00	17.3	16.7	*	1.00	20.62	5876.0	1.00	1.00	18.6	*
Mutagenesis	100	1.00	1.00	1.4	267.8	1.00	1.00	10.0	147.9	*	0.98	12.90	3867.4	0.97	0.97	10.2	*
Biopax	96	1.00	1.00	1.1	39.8	0.99	0.99	3.7	55.24	*	1.00	6.74	5691.2	0.99	0.98	3.70	*

Statistical Hypothesis Testing. We carried out a Wilcoxon signed-rank test to check whether our results are significant. Our null hypothesis was that the performances of DRILL and CELOE come from the same distribution provided that a goal state is found. The alternative hypothesis was correspondingly that these results come from different distributions. To perform the Wilcoxon signed-rank test (two-sided), we used the differences of the runtimes of DRILL and CELOE on benchmark datasets provided both approach found a goal node (F1-score 1.0). In Wilcoxon signed-rank test, we were able to reject the null hypothesis with a p-value $< 1\%$. Ergo, the superior performance of DRILL is statistically significant.

Parameter Analysis and Optimization. DRILL achieves state-of-the-art performance on all datasets without requiring extensive parameter optimization. Throughout our experiments, DRILL is trained with a fixed configuration: 32 input channels, (3x3) kernel and DRILL has only 1.3 million parameters.

Discussion Our results on all benchmark datasets suggest that DRILL achieves a state-of-the-art performance w.r.t. the quality of the concepts it generates while outperforming the state of the art significantly w.r.t. its runtime. This improvement in performance is due to the following: (i) deep Q-learning, (ii) the length-based refinement operator and (iii) the efficient computation of heuristic values. Deep Q-learning endows DRILL with the ability of considering future rewards while selecting the next state for the refinement. State-of-the-art approaches lack this ability. When using a myopic reward function, our refinement operator would lead to more refinements being considered than a subsumption-based refinement operator. However, using a length-based refinement operator allows DRILL to detect redundant states. This ability results in reducing number of times the refinement operator applied during the search. In our experimental setting, we observe that DRILL is able to estimate promises of more than 10^3 states less than a second on standard hardware.

8 Conclusion and Future Work

In this work, we introduced DRILL—a novel class expression learning approach that leverages a convolutional deep Q-network to accelerate the learning of concepts in \mathcal{ALC} . To our knowledge, DRILL is the first deep reinforcement model that is used to learn class expressions in \mathcal{ALC} . By virtue of using reinforcement learning, DRILL is endowed with the capability of incorporating information pertaining to future rewards while determining the heuristic value of states. CEL approaches lack this ability as they rely on myopic heuristic functions to guide their search through an infinite concept space. Our experiments show that DRILL outperforms state-of-the-art approaches w.r.t. its runtime. Our statistical hypothesis test confirms the superior performance of DRILL on all benchmark datasets.

In future work, we plan to investigate: (i) learning embeddings during the training phase, (ii) using LSTM and Transformer architecture in DRILL, (iii) constructing a reward function based on the gain function in DL-FOIL, and (iv) leveraging reinforcement learning at generating difficult learning problems.

References

1. Badea, L., Nienhuys-Cheng, S.H.: A refinement operator for description logics. In: Cussens, J., Frisch, A. (eds.) *Inductive Logic Programming*. pp. 40–59. Springer Berlin Heidelberg, Berlin, Heidelberg (2000)
2. Bin, S., Bühmann, L., Lehmann, J., Ngomo, A.C.N.: Towards sparql-based induction for large-scale rdf data sets. In: *Proceedings of the Twenty-second European Conference on Artificial Intelligence*. pp. 1551–1552. IOS Press (2016)
3. Bordes, A., Chopra, S., Weston, J.: Question answering with subgraph embeddings. arXiv preprint arXiv:1406.3676 (2014)
4. Bühmann, L., Lehmann, J., Westphal, P.: DL-learner—a framework for inductive learning on the semantic web. *Journal of Web Semantics* **39**, 15–24 (2016)
5. Burnett, M.: Explaining ai: fairly? well? In: *Proceedings of the 25th International Conference on Intelligent User Interfaces*. pp. 1–2 (2020)
6. Chan, C.W., Farias, V.F.: Stochastic depletion problems: Effective myopic policies for a class of dynamic optimization problems. *Mathematics of Operations Research* **34**(2), 333–350 (2009)
7. Cohen, W.W., Borgida, A., Hirsh, H.: Computing least common subsumers in description logics. In: *AAAI* (1992)
8. Das, R., Dhuliawala, S., Zaheer, M., Vilnis, L., Durugkar, I., Krishnamurthy, A., Smola, A., McCallum, A.: Go for a walk and arrive at the answer: Reasoning over paths in knowledge bases using reinforcement learning. In: *6th International Conference on Learning Representations, ICLR 2018, Vancouver, BC, Canada, April 30 - May 3, 2018, Conference Track Proceedings*. OpenReview.net (2018)
9. Demir, C., Moussallem, D., Ngomo, A.C.N.: A shallow neural model for relation prediction. In: *2021 IEEE 15th International Conference on Semantic Computing (ICSC)*. pp. 179–182. IEEE (2021)
10. Demir, C., Ngomo, A.C.N.: Convolutional complex knowledge graph embeddings. In: *Eighteenth Extended Semantic Web Conference - Research Track* (2021)

11. Doshi-Velez, F., Kim, B.: Towards a rigorous science of interpretable machine learning. arXiv preprint arXiv:1702.08608 (2017)
12. Eder, J.S.: Knowledge graph based search system (2012), US Patent App. 13/404,109
13. Edwards, A.D., Sahni, H., Liu, R., Hung, J., Jain, A., Wang, R., Ecoffet, A., Miconi, T., Isbell, C., Yosinski, J.: Estimating $q(s, s')$ with deep deterministic dynamics gradients. In: Proceedings of the 37th International Conference on Machine Learning, ICML 2020, 13–18 July 2020, Virtual Event. Proceedings of Machine Learning Research, vol. 119, pp. 2825–2835. PMLR (2020)
14. Fanizzi, N., d’Amato, C., Esposito, F.: DL-foil concept learning in description logics. In: International Conference on Inductive Logic Programming. pp. 107–121. Springer (2008)
15. Fanizzi, N., Rizzo, G., d’Amato, C.: Boosting dl concept learners. In: European Semantic Web Conference. pp. 68–83. Springer (2019)
16. Hogan, A., Blomqvist, E., Cochez, M., d’Amato, C., de Melo, G., Gutierrez, C., Gao, J.E.L., Kirrane, S., Neumaier, S., Polleres, A., et al.: Knowledge graphs. arXiv preprint arXiv:2003.02320 (2020)
17. Holzinger, A., Langs, G., Denk, H., Zatloukal, K., Müller, H.: Causability and explainability of artificial intelligence in medicine. Wiley Interdisciplinary Reviews: Data Mining and Knowledge Discovery **9**(4), e1312 (2019)
18. Iannone, L., Palmisano, I., Fanizzi, N.: An algorithm based on counterfactuals for concept learning in the semantic web. Applied Intelligence **26**(2), 139–159 (2007)
19. Lehmann, J.: Learning OWL class expressions, vol. 22. IOS Press (2010)
20. Lehmann, J., Auer, S., Bühmann, L., Tramp, S.: Class expression learning for ontology engineering. Journal of Web Semantics **9**(1), 71–81 (2011)
21. Lehmann, J., Fanizzi, N., Bühmann, L., d’Amato, C.: Concept learning. Perspectives on ontology learning **18**, 71–91 (2014)
22. Lehmann, J., Hitzler, P.: A refinement operator based learning algorithm for the *alc* description logic. In: International Conference on Inductive Logic Programming. pp. 147–160. Springer (2007)
23. Lehmann, J., Hitzler, P.: Concept learning in description logics using refinement operators. Machine Learning **78**(1–2), 203 (2010)
24. Lin, X.V., Socher, R., Xiong, C.: Multi-hop knowledge graph reasoning with reward shaping. In: Proceedings of the 2018 Conference on Empirical Methods in Natural Language Processing. pp. 3243–3253. Association for Computational Linguistics, Brussels, Belgium (2018)
25. Malyshev, S., Krötzsch, M., González, L., Gonsior, J., Bielefeldt, A.: Getting the most out of wikidata: semantic technology usage in wikipedia’s knowledge graph. In: International Semantic Web Conference. pp. 376–394. Springer (2018)
26. Mnih, V., Kavukcuoglu, K., Silver, D., Rusu, A.A., Veness, J., Bellemare, M.G., Graves, A., Riedmiller, M., Fidjeland, A.K., Ostrovski, G., et al.: Human-level control through deep reinforcement learning. nature **518**(7540), 529–533 (2015)
27. Moussallem, D., Ngonga Ngomo, A.C., Buitelaar, P., Arcan, M.: Utilizing knowledge graphs for neural machine translation augmentation. In: Proceedings of the 10th International Conference on Knowledge Capture. pp. 139–146. K-CAP ’19, ACM, New York, NY, USA (2019)
28. Ngonga Ngomo, A.C., Moussallem, D., Bühmann, L.: A holistic natural language generation framework for the semantic web. arXiv e-prints pp. arXiv–1911 (2019)
29. Saleem, M., Kamdar, M.R., Iqbal, A., Sampath, S., Deus, H.F., Ngonga Ngomo, A.C.: Big linked cancer data: Integrating linked tcga and pubmed. Journal of web semantics **27**, 34–41 (2014)

30. Samek, W.: Explainable AI: interpreting, explaining and visualizing deep learning, vol. 11700. Springer Nature (2019)
31. Samek, W., Müller, K.R.: Towards explainable artificial intelligence. In: Explainable AI: interpreting, explaining and visualizing deep learning, pp. 5–22. Springer (2019)
32. Samek, W., Wiegand, T., Müller, K.R.: Explainable artificial intelligence: Understanding, visualizing and interpreting deep learning models. arXiv preprint arXiv:1708.08296 (2017)
33. Silver, D., Huang, A., Maddison, C.J., Guez, A., Sifre, L., van den Driessche, G., Schrittwieser, J., Antonoglou, I., Panneershelvam, V., Lanctot, M., Dieleman, S., Grewe, D., Nham, J., Kalchbrenner, N., Sutskever, I., Lillicrap, T., Leach, M., Kavukcuoglu, K., Graepel, T., Hassabis, D.: Mastering the game of go with deep neural networks and tree search. *Nature* **529**, 484–503 (2016)
34. Sutton, R.S., Barto, A.G.: Reinforcement learning: An introduction. MIT press (2018)
35. Xian, Y., Fu, Z., Muthukrishnan, S., de Melo, G., Zhang, Y.: Reinforcement knowledge graph reasoning for explainable recommendation. In: Piwowarski, B., Chevalier, M., Gaussier, É., Maarek, Y., Nie, J., Scholer, F. (eds.) Proceedings of the 42nd International ACM SIGIR Conference on Research and Development in Information Retrieval, SIGIR 2019, Paris, France, July 21–25, 2019. pp. 285–294. ACM (2019)
36. Xiong, W., Hoang, T., Wang, W.Y.: DeepPath: A reinforcement learning method for knowledge graph reasoning. In: Proceedings of the 2017 Conference on Empirical Methods in Natural Language Processing. pp. 564–573. Association for Computational Linguistics, Copenhagen, Denmark (2017)
37. Zhang, F., Yuan, N.J., Lian, D., Xie, X., Ma, W.Y.: Collaborative knowledge base embedding for recommender systems. In: KDD. pp. 353–362. ACM (2016)
38. Zheng, G., Zhang, F., Zheng, Z., Xiang, Y., Yuan, N.J., Xie, X., Li, Z.: DRN: A deep reinforcement learning framework for news recommendation. In: Champin, P., Gandon, F.L., Lalmas, M., Ipeirotis, P.G. (eds.) Proceedings of the 2018 World Wide Web Conference on World Wide Web, WWW 2018, Lyon, France, April 23–27, 2018. pp. 167–176. ACM (2018)